Growth/differentiation factor 3 signals through ALK7 and regulates accumulation of adipose tissue and diet-induced obesity

Olov Andersson*, Marion Korach-Andre†, Eva Reissmann*, Carlos F. Ibáñez*‡, and Philippe Bertolino*

*Division of Molecular Neurobiology, Department of Neuroscience, Karolinska Institutet, S-17177 Stockholm, Sweden; and †Receptor Biology Unit, Department of Biosciences and Nutrition, Karolinska Institutet NOVUM, S-14157 Huddinge, Sweden

Growth/differentiation factor 3 (GDF3) is highly expressed in adipose tissue, and previous overexpression experiments in mice have suggested that it may act as an adipogenic factor under conditions of high lipid load. GDF3 has been shown to signal via the activin receptor ALK4 during embryogenesis, but functional receptors in adipose tissue are unknown. In this study, we show that $Gdf3^{-/-}$ mutant mice accumulate less adipose tissue than WT animals and show partial resistance to high-fat diet-induced obesity despite similar food intake. We also demonstrate that GDF3 can signal via the ALK4-homolog ALK7 and the coreceptor Cripto, both of which are expressed in adipose tissue. In agreement with a role for ALK7 in GDF3 signaling *in vivo*, mutant mice lacking ALK7 also showed reduced fat accumulation and partial resistance to diet-induced obesity. We propose that GDF3 regulates adipose-tissue homeostasis and energy balance under nutrient overload in part by signaling through the ALK7 receptor.

high-fat diet | metabolism | TGF-β | energy balance | insulinemia

Long regarded as no more than an energy storage depot, adipose tissue has more recently emerged as an important regulator of metabolic homeostasis through the synthesis and release of peptide hormones by adipocytes, generally known as adipokines (1). Because of the prominent role of adipose tissue in several human metabolic disorders, such as obesity and diabetes, the identification and characterization of adipokines is crucially important for our understanding of the role of adipose tissue as an integrator of homeostatic processes. Several members of the transforming growth factor-β (TGF-β) superfamily of ligands—a structurally related but functionally heterogeneous group of cytokines that includes TGF-βs, activins, bone morphogenetic proteins (BMPs) and growth/differentiation factors (GDFs)—are expressed in adipocytes, where they appear to have functions related to adipocyte differentiation. TGF-β1 has been shown to block preadipocyte differentiation *in vitro* (2), and transgenic overexpression of TGF-β1 in mice led to lipodystrophy (3). The TGF-β protein myostatin, also known as GDF8, has been shown to regulate adipogenesis *in vitro* either directly or indirectly by blocking BMP signaling (4, 5). In agreement with a role in adipocyte differentiation, targeted ablation of myostatin in mice reduced accumulation of adipose tissue and weight gain in mouse models of obesity (6). It is, however, less clear whether TGF-β superfamily proteins can regulate mature adipocyte function in addition to differentiation.

Growth/differentiation factor 3 (GDF3, also called Vgr-2) is most prominently expressed in adult adipose tissue (7, 8), and an earlier study found *Gdf3* expression to be markedly increased in an obese-mouse model lacking adipocyte fatty acid-binding protein (FABP4/aP2) (9). GDF3 overexpression in mice by adenovirus gene transfer resulted in increased adipose-tissue mass and weight gain under a high-fat diet but had no effect in a normal chow diet (10), suggesting that GDF3 may act as an adipogenic factor under a high lipid load. However, whether endogenous GDF3 has any physiological function in adipose

tissue and metabolic control has remained unknown. During embryogenesis, GDF3 has been shown to signal through a receptor complex comprising the activin type I receptor ALK4, type II receptors ActRIIA or B, and the coreceptor Cripto to control formation of anterior visceral endoderm and mesoderm (11, 12). The receptors that mediate the functions of GDF3 in the adult have not been characterized.

We and others have recently shown that inactivation of the *Gdf3* gene in mice leads to embryonic lethality in one-third of the mutant embryos because of pregastrulation developmental malformations (11, 12). However, the majority of *Gdf3* mutants survive until adulthood without any overt abnormality. In this study, we used these mice to investigate the requirement of GDF3 for adipose-tissue homeostasis under normal and high-fat diet regimes and elucidated a previously unknown receptor complex for GDF3 based on the type I receptor ALK7 that is likely involved in the effects of this cytokine in adult adipose tissue.

Results

Gdf3$^{-/-}$ Mutant Mice Gain Less Weight During Diet-Induced Obesity Despite Normal Food Intake.
The growth of WT and $Gdf3^{-/-}$ mutant mice fed normal chow or a high-fat diet was monitored between 2 and 5 months of age. No significant differences were observed on chow (Fig. 1A). In contrast, a significant difference in body weight was found after 5 weeks into a high-fat diet that persisted and increased over time (Fig. 1B). After 14 weeks on a high-fat diet, the average weight increase for WT mice was 17.1 g but only 13.1 g for $Gdf3^{-/-}$ mutants, a decrease in weight gain of 23% (Fig. 1B). This difference was not due to reduced food intake, because WT and $Gdf3^{-/-}$ mice consumed comparable amounts of food during this period (Fig. 1C). The reduced weight gain of $Gdf3^{-/-}$ mutants despite equal energy intake indicates that GDF3 is involved in the regulation of energy balance in mice.

Reduced Accumulation of Adipose Tissue in Mice Lacking GDF3.
To determine whether the reduction in weight gain observed in $Gdf3^{-/-}$ mice was due to a reduced accumulation of fat, we examined adipose tissues in WT and mutant mice after 14 weeks on chow or high-fat diets by using different approaches. The epididymal fat pads were significantly smaller in *Gdf3* mutants under both the normal and high-fat diet regimes (Fig. 2A). In agreement with this observation, histological analysis of paraffin sections from epididymal fat pads revealed a marked decrease in
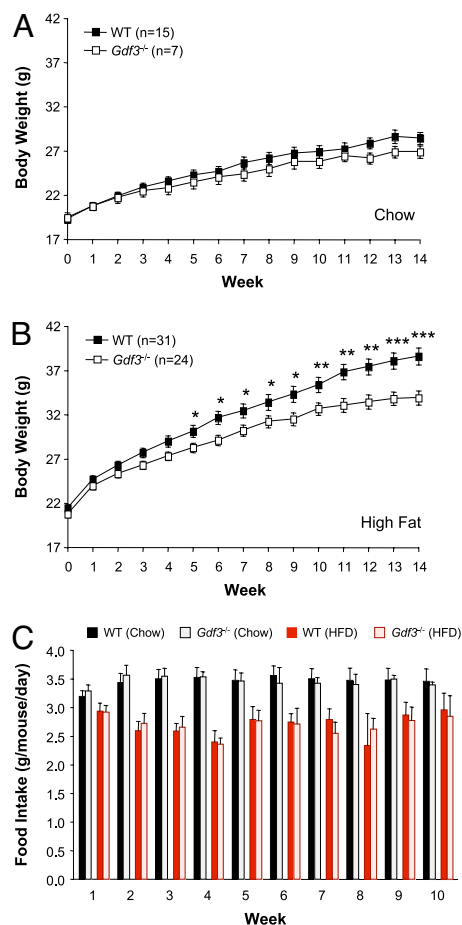
Fig. 1. *Gdf3*⁻/⁻ mutant mice gain less weight during diet-induced obesity despite normal food intake. (*A* and *B*) Body weight of 2-month-old WT and *Gdf3*⁻/⁻ mutant mice that were fed on a normal chow diet was monitored during subsequent 14 weeks on either chow (*A*) or a high-fat diet (HFD) (*B*). No significant differences were found in chow diet. (*C*) Weekly food consumption measured from four independent cages per genotype during the first 10 weeks of the period shown in *A* and *B*. Results are shown as mean ± SEM. *, P < 0.05; **, P < 0.01; ***, P < 0.001 (Student's *t* test).

Fig. 2. Reduced accumulation of adipose tissue in mice lacking GDF3. (*A*) Weight of epididymal fat pads of 5-month-old mice on a chow diet (WT, n = 28; *Gdf3*⁻/⁻, n = 16), or after 14 weeks of a high-fat diet (WT, n = 50; *Gdf3*⁻/⁻, n = 29). (*B*) Histological analysis of paraffin sections from epididymal fat pads of WT and *Gdf3*⁻/⁻ mice by H&E staining. (Scale bar, 100 μm.) (*C*) Representative MRI images of 5-month old WT and *Gdf3*⁻/⁻ mutant mice fed a chow diet or after 14 weeks on a high-fat diet. (*D*) Quantification of total fat content by MRI (chow, n = 5 per genotype; high-fat diet, n = 13 per genotype). Results are expressed as mean ± SEM. *, P < 0.05; **, P < 0.01 vs. WT (Student's *t* test).

adipocyte cell size in *Gdf3*⁻/⁻ mice compared with WT controls under both diet regimes (Fig. 2*B*). Total body fat was then investigated by using MRI, which revealed reductions in both visceral and subcutaneous fat depots in the mutants (Fig. 2*C*). Quantification of total body fat from MRI scans showed that *Gdf3*⁻/⁻ mice had on average 44% and 28% less body fat than WT controls after 14 weeks on chow and high-fat diet, respectively (Fig. 2*D*). At the end of 14 weeks on the high-fat diet, the mutants accumulated 2.5 g less of fat than WT controls, which accounts for ≈60% of their reduction in body weight.

Expression and Functional Characterization of a GDF3 Receptor Complex Based on the Type I Receptor ALK7. GDF3 has been shown to directly bind and signal through a receptor complex consisting of a type I receptor (the activin receptor ALK4), a type II receptor (either ActRIIA or -B), and the GPI-anchored coreceptor Cripto (11, 12). The dependence of GDF3 signaling on the presence of Cripto resembles the signaling mechanism used by two other TGF-β superfamily ligands, namely Nodal and GDF1 (13–15). Because both Nodal and GDF1 have also been shown to signal via the related type I receptor ALK7 (13, 16), we speculated that GDF3 may also be able to signal via ALK7 in the presence of Cripto. We first investigated the expression of

candidate receptor components in adipose tissue by RT-PCR using RNA isolated from visceral fat of WT, *Gdf3*⁻/⁻, and *Alk7*⁻/⁻ mice. This analysis confirmed expression of *Gdf3*, *Alk7*, *Alk4*, *ActRII-A*, *ActRII-B*, and *Cripto* in adipose tissue from WT animals (Fig. 3*A*). We then investigated whether GDF3 may signal through a receptor complex including ALK7 by transient transfection in heterologous cells by using a gene reporter construct based on a promoter element (CAGA-luc) that reports activation of Smad3, a key downstream mediator of TGF-β superfamily signaling (17). R4-2 cells express low levels of type I receptors, but normal levels of type II receptors, and are therefore well suited for functional analysis of exogenous type I receptor molecules. In the presence of both ALK7 and Cripto, GDF3 could robustly activate the CAGA-luc reporter in R4-2 cells (Fig. 3*B*). A second assay was performed in HepG2 cells by using an ALK7 chimeric receptor (ALK7/3) carrying the intracellular L45 loop from the BMP receptor ALK3, which allows it to activate a reporter construct carrying a BMP-responsive element (BRE-luc) (18–20). As expected, GDF3 had no effect on its own in this assay, whereas BMP4 could readily activate the reporter in the absence of any additional component (Fig. 3*C*). However, GDF3 was able to robustly activate the reporter in the presence of the ALK7/3 chimera and Cripto (Fig. 3*C*). The ability of ALK7 to mediate GDF3 signaling, together with its expression in adipose tissue along with type II receptors and Cripto, suggested that ALK7 may participate in the effects of GDF3 on energy balance and fat accumulation and prompted us to investigate whether mice lacking ALK7 display any of the phenotypes found in *Gdf3*⁻/⁻ mutants.

Reduced Diet-Induced Weight Gain and Fat Accumulation in Mice Lacking ALK7. Similar to *Gdf3*⁻/⁻ mutants, *Alk7*⁻/⁻ mice showed no difference in body weight compared with WT controls when fed normal chow (data not shown). In contrast, a significant reduction
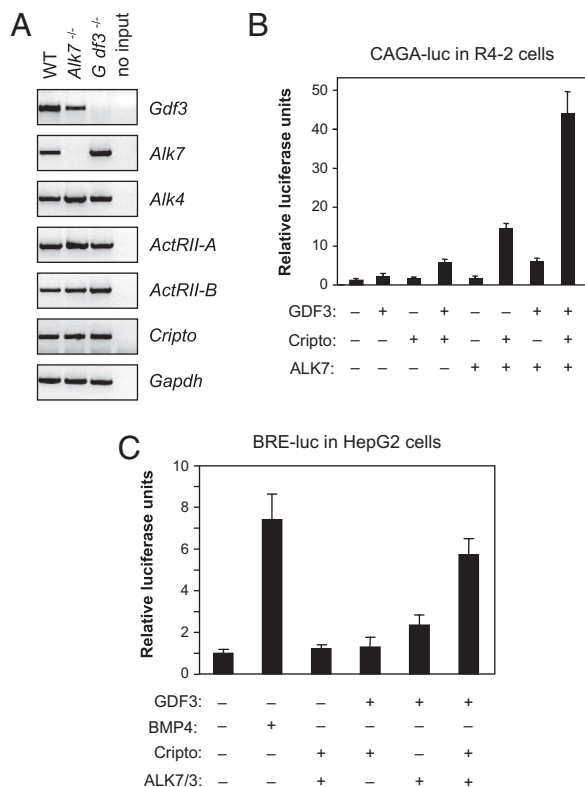
Fig. 3. *Alk7* is expressed in adipose tissue and can mediate GDF3 signaling in a Cripto dependent manner. (*A*) RT-PCR analysis of *Gdf3*, *Alk7*, *Alk4*, *ActRII-A*, *ActRII-B*, and *Cripto* mRNA expression. *Gapdh* mRNA expression is shown in the bottom-most panel as a loading control. ''no input'' indicates that no mRNA was used for RT-PCR. (*B*) Luciferase reporter assay in R4-2 cells transfected with a CAGA-luc reporter and plasmids encoding mature GDF3, ALK7, and Cripto as indicated. Results are expressed in relative luciferase units normalized to control (mean ± SD of triplicate observations). (*C*) Luciferase reporter assay in HepG2 cells transfected with a BRE-luc reporter and plasmids encoding mature GDF3, Cripto, and chimeric type I receptor ALK7/3 as indicated. BMP4 protein (50 ng/ml) was used as a positive control for reporter activation.

in weight gain was observed after 10 weeks into a high-fat diet (Fig. 4*A*). After 14 weeks on the high-fat diet, the average weight increase for WT mice was 17.2 g but only 12.2 g for $Alk7^{-/-}$ mutants, a decrease in weight gain of 29% (Fig. 4*A*). As in $Gdf3^{-/-}$ mutants, food intake was also comparable between mice lacking ALK7 and WT controls (Fig. 4*B*), suggesting abnormal energy balance in the mutants. A strong reduction in the size of epididymal fat pads was also observed in $Alk7^{-/-}$ mutants after a high-fat diet but not after a normal chow diet (Fig. 4*C*). Moreover, adipocytes in epididymal fat pads of mice lacking ALK7 were also smaller in size (Fig. 4*D*). Quantification of total body fat by MRI revealed a reduction of 25% in body fat content in $Alk7^{-/-}$ mutants after a high-fat diet (Fig. 4 *E* and *F*). No difference was found in mice fed a normal chow diet (data not shown). These data indicate that, on a high-fat diet, $Alk7^{-/-}$ mutants phenocopy the weight gain and fat-accumulation abnormalities observed in mice lacking GDF3 but appear to be less affected when fed a normal chow diet.

Mice Lacking GDF3, Unlike Those Lacking ALK7, Display Normal Insulinemia and Insulin Sensitivity. We have recently shown in a separate study that ALK7 functions as a negative regulator of insulin secretion in pancreatic islets and that mice lacking ALK7 have elevated serum insulin levels from early postnatal stages and develop reduced insulin sensitivity and liver steatosis as adults (21). It was therefore of interest to determine whether mice lacking GDF3 display similar abnormalities. Unlike

$Alk7^{-/-}$ mice, however, $Gdf3^{-/-}$ mutants showed normal serum insulin levels (Fig. 5*A*) and insulin sensitivity (Fig. 5*B*). Moreover, the liver weight of mice lacking GDF3 was similar to that of WT controls after both regular chow or high-fat diet (Fig. 5*C*). Unlike the livers of $Alk7^{-/-}$ mutants, $Gdf3^{-/-}$ livers showed no signs of elevated lipid accumulation in a normal chow diet as assessed by Oil red-O staining (Fig. 5*D*). These data suggest a more restricted role of GDF3 in the control of weight gain and buildup of adipose tissue than its receptor ALK7.
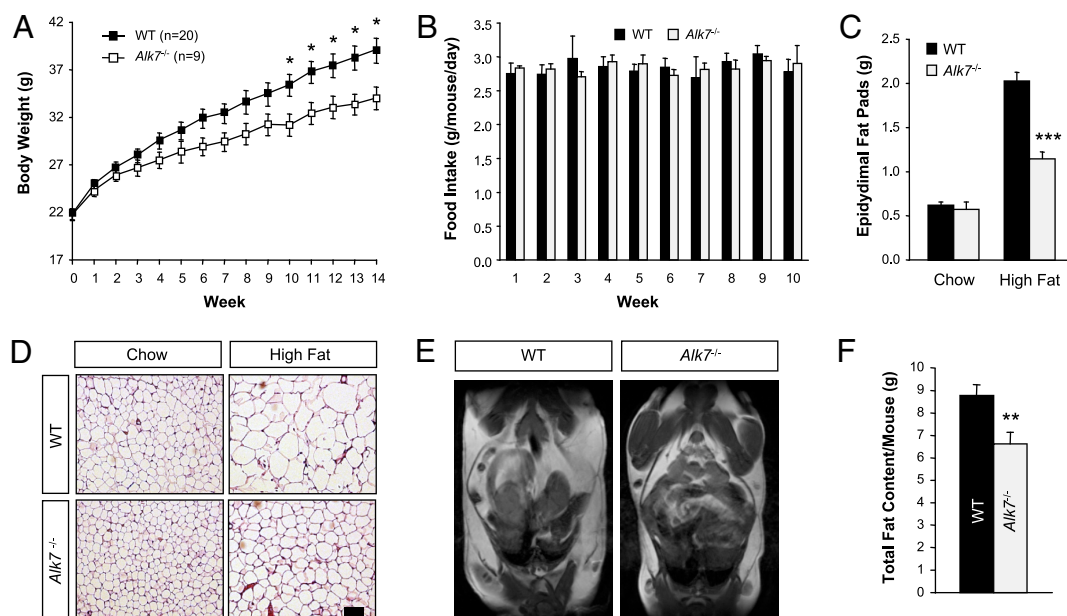
Discussion

The results of this study support a role for GDF3 as an important endogenous regulator of fat accumulation and energy balance. We also show that GDF3 is able to signal via a receptor complex based on ALK7 and Cripto, both of which are endogenously expressed in adipose tissue. In agreement with a role for ALK7 in GDF3 signaling *in vivo*, mice lacking this receptor show similar abnormalities in diet-induced fat accumulation and weight gain to those observed in $Gdf3^{-/-}$ mutants. $Alk7^{-/-}$ mice, however, display a wider range of defects than $Gdf3^{-/-}$ mutants, particularly with regard to serum insulin levels and insulin sensitivity, suggesting the involvement of other ALK7 ligands in those functions. In agreement with this, we have recently found that activin B signals through ALK7 to negatively regulate Ca^{2+} influx in pancreatic β-cells and that mice lacking activin B ($Inh\beta B^{-/-}$ mice) show hyperinsulinemia comparable with that of $Alk7^{-/-}$ mutants (21). Double mutants lacking both activin B and ALK7 showed no additive effects, suggesting that they function in a common pathway to regulate serum insulin levels. Thus, the more complex phenotype displayed by $Alk7^{-/-}$ mice may result from defects in the signaling activities of several ligands of this receptor. Interestingly, in contrast to $Alk7^{-/-}$ mice, neither $Gdf3^{-/-}$ or $Inh\beta B^{-/-}$ mutants show signs of reduced insulin sensitivity or liver steatosis (this study and ref. 21). Those phenotypes could thus be the result of defects in the activities of yet additional ALK7 ligands or, perhaps more interestingly, arise as a synergistic effect of combined hyperinsulinemia and reduced fat deposition caused by abnormalities in both activin B and GDF3 signaling. This possibility could be addressed in future studies by the generation and analysis of compound $Gdf3^{-/-};Inh\beta B^{-/-}$ double mutants. It should, however, be noted that, because of the ability of GDF3 and activin B to activate ALK4 as well as ALK7, the genetics of a signaling network with ligands that have several receptors and receptors that have multiple ligands can be complicated, and it is unlikely that compound mutations in either ligands or receptors will strictly phenocopy each other.

In a previous study, intravenous injection of an adenoviral vector driving GDF3 overexpression increased fat accumulation and weight gain in mice undergoing a high-fat diet but had no effect in animals fed normal chow, leading the authors of that study to propose that GDF3 actions may be restricted to conditions of nutrient overload (10). However, our observation that mice lacking GDF3 have less adipose tissue than WT controls even when fed regular chow indicates that GDF3 has a more general role in fat accumulation independently of the regime of energy intake. In contrast to $Gdf3^{-/-}$ mutants, $Alk7^{-/-}$ mice appeared to be less affected when fed a chow diet, suggesting that perhaps ALK4 may compensate for the lack of ALK7 under those conditions. $Alk4^{-/-}$ mutants die early in embryonic development (22) and are therefore unsuitable to assess the adult roles of this receptor. Intriguingly, one study has reported increased *Alk7* expression in cell lines after exposure to fatty acids (23), which would be in agreement with a more prominent role for ALK7 during nutrient overload.

The coexpression of GDF3 and its receptors in adipose tissue suggests that at least part of the effects of this ligand on fat cells are mediated in a paracrine fashion. Although adipose tissue is the most prominent site of GDF3 expression, this ligand has also been detected in circulation in the bloodstream (9) and may thus affect fat deposition and energy balance through non-cell-autonomous

Fig. 4. Reduced diet-induced weight gain and fat accumulation in mice lacking ALK7. (*A*) Body weight of 2-month-old WT and *Alk7*$^{-/-}$ mutant mice during subsequent 14 weeks on a high-fat diet. (*B*) Weekly food consumption measured from four independent cages per genotype during the first 10 weeks of the period shown in *A*. (*C*) Weight of epididymal fat pads of 5-months-old mice on a chow diet (WT, *n* = 25; *Alk7*$^{-/-}$, *n* = 13), or after 14 weeks of a high-fat diet (WT, *n* = 50; *Alk7*$^{-/-}$, *n* = 24). (*D*) Histological analysis of paraffin sections from epididymal fat pads of WT and *Alk7*$^{-/-}$ by H&E staining. (Scale bar, 100 μm.) (*E*) Representative MRI images of 5-month-old WT and *Alk7*$^{-/-}$ mutant mice after 14 weeks on a high-fat diet. (*F*) Quantification of total fat content by MRI (*n* = 11 for each genotype). Results are expressed as mean ± SEM. *, $P < 0.05$; **, $P < 0.01$; ***, $P < 0.001$ vs. WT (Student's *t* test).
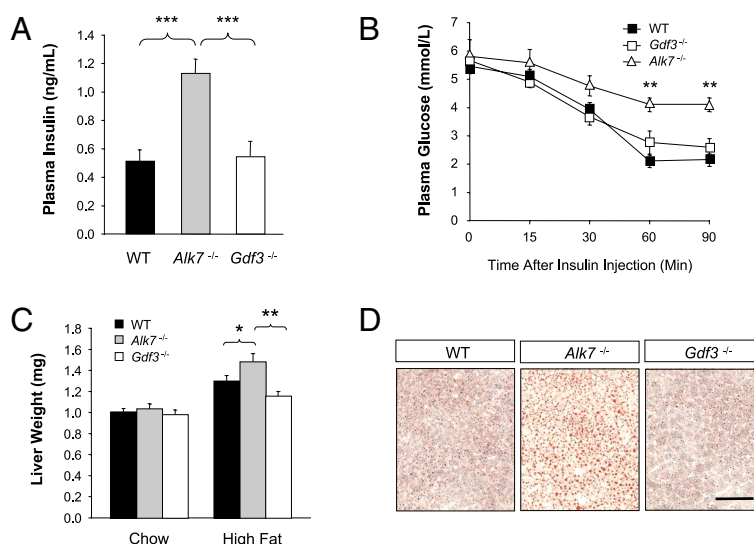
effects. The requirement for the Cripto coreceptor, which is excluded from several tissues that express other GDF3 receptor components—such as pancreatic β-cells (24), is likely to provide tissue specificity to GDF3 signaling. Future studies, including conditional inactivation, will be required to unravel tissue-specific effects of GDF3 and its receptors. From a therapeutic point of view, our results suggest that GDF3 antagonists or inhibitors may find clinical applications in the control of diet-induced obesity and fat deposition, particularly in individuals exposed to diet regimes of high caloric intake.

Materials and Methods

Fig. 5. Mice lacking GDF3, unlike those lacking ALK7, display normal insulinemia and insulin sensitivity. (*A*) Insulin serum levels after overnight fasting in 5-month-old WT (*n* = 16), *Alk7*$^{-/-}$ (*n* = 11), and *Gdf3*$^{-/-}$ (*n* = 9) mice. (*B*) Insulin tolerance test of 5-month-old WT (*n* = 9), *Alk7*$^{-/-}$ (*n* = 6), and *Gdf3*$^{-/-}$ (*n* = 9) mice maintained on chow diet. (*C*) Wet liver weight of 5-month-old WT (chow, *n* = 28; high-fat diet, *n* = 54), *Alk7*$^{-/-}$ (chow, *n* = 13; high-fat diet, *n* = 24), and *Gdf3*$^{-/-}$ (chow, *n* = 16; high-fat diet, *n* = 29) mice after being subjected to chow or high-fat diet. (*D*) Histological analysis of liver sections from 2-month-old WT, *Alk7*$^{-/-}$, and *Gdf3*$^{-/-}$ mice by Oil red-O staining. Results are shown as mean ± SEM. *, $P \leq 0.05$; **, $P < 0.01$; ***, $P < 0.001$ (Student's *t* test). (Scale bar, 100 μm.)

before subsequent tissue analyses. The composition of the high-fat diet was (in kcal%) 60% fat, 20% carbohydrate, and 20% protein. Animal protocols were approved by Stockholms Norra Djurförsöksetiska Nämnd and were in accordance with ethical guidelines of the Karolinska Institute.

Receptor Reconstitution Experiments. Receptor reconstitution and reporter gene experiments were performed in R4-2 and HepG2 cells cultured in 24-well plates, as described (13). The mature domain of GDF3 was expressed from a chimeric construct carrying a prodomain from activin B to enhance signaling strength, as described (11). The chimeric type I receptor ALK7 L45-ALK3 (ALK7/3) was generated by substituting Asn-257, Asp-259, Asn-260, and Thr-262 of ALK7 with Ile-269, Gly-271, Thr-272, and Ser-274 by site-directed mutagenesis. The amounts of plasmid DNA transfected into cells (per three wells) were as follows: 10 ng for WT ALK7, 100 ng for chimeric ALK7/3, 30 ng for Cripto, and 800 ng for GDF3.

Histological Analysis. Freshly dissected tissues were fixed in formalin before paraffin embedding and sectioning. H&E staining of sections was performed according to standard procedures. Oil red-O (Sigma–Aldrich) staining was performed on frozen liver sections by following standard protocols.

MRI Scans and Analysis. *In vivo* MRI measurements were made under 1.5–2% isoflurane in O_2 anesthesia. Fat distribution was measured in every mouse after 14 weeks on either chow or high-fat diet. All *in vivo* magnetic resonance (MR) measurements were performed on a Bruker 4.7-T field-strength magnet and a 40-cm horizontal bore diameter (Bruker Biospec Avance 47/40; Bruker) equipped with a commercially available circular resonator (Bruker) with an inner diameter of 24 mm for RF pulse application and signal detection. Body temperature was maintained by using a temperature-controlled air stream around the body of the mouse. For the measurement of whole- body adiposity, the main sequence used was a Bruker implementation of rapid acquisition with relaxation enhancement (RARE) imaging (26) as described (27). Briefly, the mouse was laid on a support and positioned in the center of the coil. A total of 40 contiguous 1.5-mm-thick transversal slices covering the mouse body were recorded. Image analysis was carried out with Paravision 2.3 image

analysis software (Bruker). MRI-visible visceral fat comprises omental, retro-peritoneal, and mesenteric fat depots. Two-dimensional image series were then imported into Biomap platform (IDL) for pixel counting-based determination of fat volumes. A signal threshold was used after applying a G filter, a maximum likelihood, and a class-select interaction to exclude all nonfat tissues in each slice. A density factor of 0.9 g/ml was used to convert fat volumes (in milliliters) into fat mass (in grams).

RT-PCR Analysis. Total RNA extraction from freshly dissected tissues was performed by TRIzol (Invitrogen) according to the manufacturer's instructions. PCR was performed by using 1 μg of reverse-transcribed cDNA (Super-Script II RT-kit; Invitrogen) and primers for *Alk7*, *Alk4*, *Gdf3*, *ActRII-A*, *ActRII-B*, *Cripto*, and *Gapdh* (primers sequences available upon request).

Metabolic Measurements. Serum insulin levels were measured in animals fasted overnight by using a mouse ELISA kit (Mercodia). Insulin tolerance tests were performed with mice starved for 3 h. Briefly, animals were given 1 unit/kg of body weight of recombinant human insulin (Actrapid; Novo Nordisk) by i.p. injection. Glucose levels were measured by tail-tip bleeding by using a FreeStyle mini Glucometer (Abbott) immediately before and 15, 30, 60, and 90 min after the insulin injection.

Statistical Analysis. Each variable was analyzed by using the unpaired Student's t test unless otherwise indicated. For all analyses, a P value of <0.05 was considered significant. Results are given as means $\pm$ SEM. All analyses were performed by using Prism4 Software (GraphPad).

1. Rosen ED, Spiegelman BM (2006) Adipocytes as regulators of energy balance and glucose homeostasis. *Nature* 444:847–853.
2. Choy L, Skillington J, Derynck R (2000) Roles of autocrine TGF-beta receptor and Smad signaling in adipocyte differentiation. *J Cell Biol* 149:667–682.
3. Clouthier DE, Comerford SA, Hammer RE (1997) Hepatic fibrosis, glomerulosclerosis, and a lipodystrophy-like syndrome in PEPCK-TGF-beta1 transgenic mice. *J Clin Invest* 100:2697–2713.
4. Feldman BJ, Streeper RS, Farese RV, Jr, Yamamoto KR (2006) Myostatin modulates adipogenesis to generate adipocytes with favorable metabolic effects. *Proc Natl Acad Sci USA* 103:15675–15680.
5. Rebbapragada A, Benchabane H, Wrana JL, Celeste AJ, Attisano L (2003) Myostatin signals through a transforming growth factor beta-like signaling pathway to block adipogenesis. *Mol Cell Biol* 23:7230–7242.
6. McPherron AC, Lee SJ (2002) Suppression of body fat accumulation in myostatin-deficient mice. *J Clin Invest* 109:595–601.
7. Jones CM, Simon-Chazottes D, Guenet JL, Hogan BL (1992) Isolation of Vgr-2, a novel member of the transforming growth factor-beta-related gene family. *Mol Endocrinol* 6:1961–1968.
8. McPherron AC, Lee SJ (1993) GDF-3 and GDF-9: Two new members of the transforming growth factor-beta superfamily containing a novel pattern of cysteines. *J Biol Chem* 268:3444–3449.
9. Witthuhn BA, Bernlohr DA (2001) Upregulation of bone morphogenetic protein GDF-3/Vgr-2 expression in adipose tissue of FABP4/aP2 null mice. *Cytokine* 14:129–135.
10. Wang W, Yang Y, Meng Y, Shi Y (2004) GDF-3 is an adipogenic cytokine under high fat dietary condition. *Biochem Biophys Res Commun* 321:1024–1031.
11. Andersson O, Bertolino P, Ibanez CF (2007) Distinct and cooperative roles of mammalian Vg1 homologs GDF1 and GDF3 during early embryonic development. *Dev Biol* 311:500–511.
12. Chen C, et al. (2006) The Vg1-related protein Gdf3 acts in a Nodal signaling pathway in the pre-gastrulation mouse embryo. *Development* 133:319–329.
13. Reissmann E, et al. (2001) The orphan receptor ALK7 and the Activin receptor ALK4 mediate signaling by Nodal proteins during vertebrate development. *Genes Dev* 15:2010–2022.
14. Cheng SK, Olale F, Bennett JT, Brivanlou AH, Schier AF (2003) EGF-CFC proteins are essential coreceptors for the TGF-beta signals Vg1 and GDF1. *Genes Dev* 17:31–36.
15. Yeo C, Whitman M (2001) Nodal signals to Smads through Cripto-dependent and Cripto-independent mechanisms. *Mol Cell* 7:949–957.
16. Andersson O, Reissmann E, Jornvall H, Ibanez CF (2006) Synergistic interaction between Gdf1 and Nodal during anterior axis development. *Dev Biol* 293:370–381.
17. Dennler S, et al. (1998) Direct binding of Smad3 and Smad4 to critical TGF beta-inducible elements in the promoter of human plasminogen activator inhibitor-type 1 gene. *EMBO J* 17:3091–3100.
18. Chen YG, et al. (1998) Determinants of specificity in TGF-beta signal transduction. *Genes Dev* 12:2144–2152.
19. Persson U, et al. (1998) The L45 loop in type I receptors for TGF-beta family members is a critical determinant in specifying Smad isoform activation. *FEBS Lett* 434:83–87.
20. Hata A, et al. (2000) OAZ uses distinct DNA- and protein-binding zinc fingers in separate BMP-Smad and Olf signaling pathways. *Cell* 100:229–240.
21. Bertolino P, et al. (2008) Activin B receptor ALK7 is a negative regulator of pancreatic β-cell function. *Proc Natl Acad Sci USA* 105:7246–7251.
22. Gu Z, et al. (1998) The type I activin receptor ActRIB is required for egg cylinder organization and gastrulation in the mouse. *Genes Dev* 12:844–857.
23. Zhang N, et al. (2006) Activin receptor-like kinase 7 induces apoptosis of pancreatic beta cells and beta cell lines. *Diabetologia* 49:506–518.
24. Zhang YQ, et al. (2004) Inhibition of activin signaling induces pancreatic epithelial cell expansion and diminishes terminal differentiation of pancreatic beta-cells. *Diabetes* 53:2024–2033.
25. Jornvall H, Reissmann E, Andersson O, Mehrkash M, Ibanez CF (2004) ALK7, a receptor for nodal, is dispensable for embryogenesis and left–right patterning in the mouse. *Mol Cell Biol* 24:9383–9389.
26. Hennig J, Nauerth A, Friedburg H (1986) RARE imaging: A fast imaging method for clinical MR. *Magn Reson Med* 3:823–833.
27. Korach-Andre M, et al. (2005) Relationship between visceral adiposity and intramyocellular lipid content in two rat models of insulin resistance. *Am J Physiol* 288:E106–E116.